Carbohydrate Polymers 91 (2013) 14–21

Contents lists available at SciVerse ScienceDirect

Carbohydrate Polymers

journal homepage: www.elsevier.com/locate/carbpol

Characterization of conducting cellulose acetate based polymer electrolytes doped with "green" ionic mixture

S. Ramesh [a,*], R. Shanti [a], Ezra Morris [b]

[a] Centre for Ionics University of Malaya, Department of Physics, Faculty of Science, University of Malaya, 50603 Kuala Lumpur, Malaysia
[b] Faculty of Engineering and Science, Universiti Tunku Abdul Rahman, 53300 Kuala Lumpur, Malaysia

ARTICLE INFO

Article history:
Received 28 May 2012
Received in revised form 25 June 2012
Accepted 2 July 2012
Available online 31 July 2012

Keywords:
DES
Ionic conductivity
Complexation
Amorphous region
Li^+ mobility

ABSTRACT

Polymer electrolytes were developed by solution casting technique utilizing the materials of cellulose acetate (CA), lithium bis(trifluoromethanesulfonyl)imide (LiTFSI) and deep eutectic solvent (DES). The DES is synthesized from the mixture of choline chloride and urea of 1:2 ratios. The increasing DES content well plasticizes the CA:LiTFSI:DES matrix and gradually improves the ionic conductivity and chemical integrity. The highest conducting sample was identified for the composition of CA:LiTFSI:DES (28 wt.%:12 wt.%:60 wt.%), which has the greatest ability to retain the room temperature ionic conductivity over the entire 30 days of storage time. The changes in FTIR cage peaks upon varying the DES content in CA:LiTFSI:DES prove the complexation. This complexation results in the collapse of CA matrix crystallinity, observed from the reduced intensity of XRD diffraction peaks. The DES-plasticized sample is found to be more heat-stable compared to pure CA. Nevertheless, the addition of DES diminishes the CA:LiTFSI matrix's heat-resistivity but at the minimum addition the thermal stability is enhanced.

1. Introduction

In recent years, we are frequently being exposed to the awareness of "green" technology with plenty of informative sources. This consciousness was brought forward by keeping in mind the critical environmental problem associated with the utilization of synthetic polymer in the production of polymer electrolytes. The growing needs of polymer electrolytes to be used in a variety of electrochemical devices (Armand, 1986; Rajendran, Sivakumar, & Subadevi, 2004; Ratner & Shriver, 1988; Shriver et al., 1981; Siva Kumar, Subrahmanyam, Jaipal Reddy, & Subba Rao, 2006), especially in lithium polymer cells, urging for better development that are more environmental friendly. In conjunction to this, the natural types of polymers have been substituted with the synthetic types.

In this research work, cellulose acetate (CA) was chosen to build up the conducting membrane. CA has number of outstanding properties as listed are; (1) non-toxic nature, (2) availability of renewable resources, (3) low cost and (4) biodegradable (Averous, Fringant, & Moro, 2001; Wu, Wang, Li, Li, & Wang, 2009). The presence of polar functional groups in its polymer chain is an added advantage, which has high affinity towards the lithium ions and plasticizing solvents (Ramesh & Lu, 2008). Up to date not much efforts were executed by researchers to develop the conducting membrane using the CA. The main obstacle that limits its wide utilization is attributed to its highly crystalline nature, which provokes the CA membrane to be insulated.

In the effort to overcome the above mentioned limitation, incorporation of suitable additives is potential to convert the highly crystalline region in CA matrix to amorphous for better ion conduction. As in this research, the initial approach to suppress the high crystallinity is done by embedding a type of ionic salt, LiTFSI into the CA matrix. This type of ionic salt is of special interest due to its large electronegativity and delocalization of charge (Ramesh & Lu, 2008). These successive properties contribute to the complete dissociation of LiTFSI in CA matrix forming free ions and retain in its ionic state throughout. The cations (Li^+) will move along the polar functional group in CA matrix whereas the anions ($TFSI^-$) modify the phase composition, both of these different charged ions exert significant influence in ionic conductivity (Ramesh, Tai, & Chia, 2008).

Further enhancement in ionic conductivity was done by incorporating DES in CA:LiTFSI matrix. The DES is a type of ionic liquid but since it is composed of a mixture of quaternary ammonium salt and hydrogen bond donors (Abbott, Capper, Davies, Rasheed, & Tambyrajah, 2003) the term ionic mixture was adopted (Hou et al., 2008). In this present work, we synthesized an ionic solvent from the eutectic mixture of choline chloride and urea (Abbott et al., 2003). This type of ionic mixture gains interest due to its

* Corresponding author. Tel.: +60 3 79674391.
E-mail addresses: rameshtsubra@gmail.com (S. Ramesh), shanthy87@yahoo.com (R. Shanti), ezram@utar.edu.my (E. Morris).

0144-8617/$ – see front matter © 2012 Elsevier Ltd. All rights reserved.
http://dx.doi.org/10.1016/j.carbpol.2012.07.061

Table 1
The composition ratio of the designated CA:LiTFSI:DES polymer electrolytes.

Designation	Polymer electrolyte composition (CA:LiTFSI:DES) (wt.%)
Pure CA	100:0:0
CA-0	70:30:0
CA-20	56:24:20
CA-40	42:18:40
CA-60	28:12:60

unique properties including; (1) unusual solvent property that further dissolves the highly crystalline CA, (2) cheap in cost compared to pure ionic liquid due to the low cost of raw materials, (3) ease in the preparation method ignoring the purification process and no medium being required, (4) most of the formulations are non-toxic and (5) biodegradable (Hou et al., 2008; Jhong, Wong, Wan, Wang, & Wei, 2009; Zhang, Wu, Chen, Feng, & Bu, 2009).

The DES do possess an unusual solvent property owing to its high chloride ion concentration and its specific activity which is capable of breaking the bonding network between the oxygen (—O) and acetate (—Ac) atom in —OAc functional group. The bond disruption causes the oxygen atom to be unoccupied, thus permitting the Li^+ ions mobility by forming a temporary co-ordination (Swatloski, Spear, Holbrey, & Rogers, 2002). Moreover, the incorporation of DES also displays high ionic conductivity as a result of its high mobility and high concentration of carrier ions (Abbott et al., 2003).

In this communication, we study the plasticizing efficiency of DES content in tailoring the insulating property of CA:LiTFSI polymer electrolytes by using various characterization techniques, namely ionic conductivity, complexation, structural conversion and thermal properties.

2. Experimental

2.1. Materials

The chemicals used to build up the non-plasticized matrix are cellulose acetate, CA (M_w = 61,000 g mol^{-1}) and lithium bis(trifluoromethanesulfonyl)imide, LiTFSI, which were purchased from Aldrich and Fluka respectively. For the matrix plasticization, DES is synthesized using the starting materials of choline chloride and urea that were procured from Sigma. The N,N-dimethylformamide, DMF solvent that purchased from R&M Chemicals is used to prepare the polymer electrolytes solution.

2.2. Preparation of polymer electrolytes

2.2.1. Synthesizing method of DES

As an initial step, an appropriate amount of choline chloride and urea in 1:2 ratio was weighed in a small glass beaker. Then, the physically mixed solid state chemicals were heated up to a temperature of 50 °C, under a manual stirring using glass rod. The synthesis process is accomplished upon the complete dissolution of the solids mixture, which produces colorless viscous solution.

2.2.2. Thin film preparation

The DES plasticized matrix was prepared by dissolving an appropriate DES composition, as shown in Table 1, into the CA:LiTFSI matrix in the presence of 10 ml DMF. Then, the solution is stirred overnight to obtain a colorless homogeneous solution. The procedure continues by spreading the suspension on a clean Petri dish and left to dry in the oven at 55 °C. Upon casting, a mechanically stable and free standing transparent thin film is obtained. The casted thin films are stored in desiccator when not in use. This is to avoid the thin films from absorbing the moisture from air since it is made of hygroscopic materials. The ratio of CA:LiTFSI is fixed at 70:30 throughout the sample composition since this is the ratio combination that gives good property for the non-plasticized matrix in terms of its conducting nature and thermal profile.

2.3. Characterization technique

The developed DES-plasticized matrix is characterized in terms of electrical, structural and thermal properties.

2.3.1. Electrical characterization

2.3.1.1. Impedance spectroscopy. This analysis is performed by using the impedance spectrometer, which tests on the ionic conductivity of samples of freshly casted and aged. The ionic conductivity of the aged samples is studied for the storage time of 30 days with every measurement recorded with 10 days interval at room temperature.

Prior testing, the thickness of the thin films is measured by using the micrometer screw gauge. Then, the thin films with the known thickness are sandwiched between two stainless steel blocking electrodes (area of 4.9807 cm^2) and tested using the HIOKI Model 3532-50 Hi-Tester. The measurements were recorded at room temperature over the frequency ranging from 50 Hz to 5 MHz with the amplitude of 10 mV.

The obtained impedance plot was used to find the bulk resistance (R_b) value to calculate the exerted ionic conductivity by substituting in Eq. (1):

$$\sigma = \frac{L}{R_b A} \quad (1)$$

where σ is the conductivity in S cm^{-1}, L refers to the thickness of thin film sample in cm, R_b is the bulk resistance in Ω obtained from Cole–Cole impedance plot whereas A represents the surface area of the stainless-steel blocking electrodes in cm^2.

2.3.2. Structural characterization

2.3.2.1. Fourier transform infrared (FTIR)-horizontal attenuated total reflection (HATR) analysis. The occurrence of complexation between the added chemical constituents in the matrix was analyzed by using Perkin–Elmer FTIR Spectrometer, Spectrum RX1, with the aid of HATR compartment. The FTIR spectra were recorded in the transmittance mode in the wave region ranging from 4000 to 600 cm^{-1} with the resolution of 4 cm^{-1}.

2.3.2.2. X-ray diffraction (XRD) analysis. The structural alternations in the CA matrix upon doping with increasing DES content are studied using the Siemens D-5000 Diffraction System with the Cu-K_α radiation of 1.5406 Å wavelength. The XRD patterns were recorded at the Bragg angles (2θ) ranging from 5° to 80° at room temperature.

2.3.3. Thermal characterization

2.3.3.1. Thermogravimetric analysis (TGA). Mettler Toledo analyzer that consist of TGA/SDTA851^e main unit and STARe software was used to analyze the thermal properties of polymer electrolytes. This analysis was performed on an approximate polymer electrolyte weight of 5 mg at the temperature ranging from 25 °C to 550 °C with the heating rate of 10 °C min^{-1} under nitrogen atmosphere.

3. Results and discussion

3.1. Ionic conductivity studies

The influence of DES content on the electrical properties of CA:LiTFSI:DES was evaluated over the storage period of 30 days and the variations are as presented in Fig. 1.

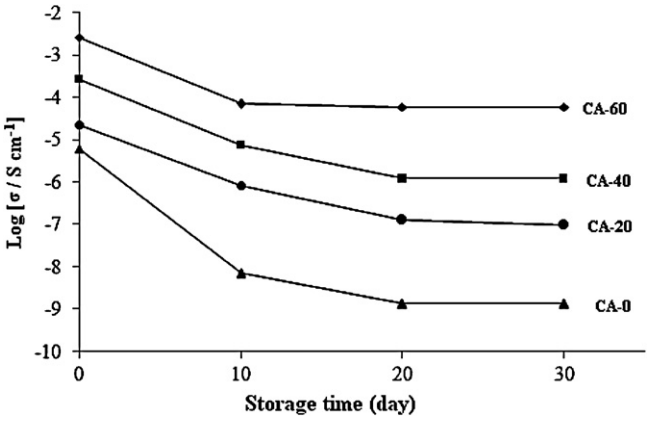

Fig. 1. Variation of log ionic conductivity with storage time for samples CA-0, CA-20, CA-40 and CA-60.

3.1.1. Different DES content doping

Focusing on the ionic conductivity variation of freshly casted samples in Fig. 1, it is noted that the ionic conductivity increases with increasing DES plasticization. This observation is rationalized by the collapse in the CA matrix crystallinity upon breaking of bonding between the oxygen (—O) and acetate (—Ac) atom in —OAc functional group, thus inducing increase in the samples amorphous nature. The increase in amorphous region signifies the increase in the number of vacant oxygen that assists in lithium conducting ions (Li^+) mobility by forming temporary ionic interaction. This interaction endorses continuous Li^+ ion hopping along the polymer backbone and subsequently enhances the ionic conductivity (Uma, Mahalingam, & Stimming, 2003).

The unusual solvent property possessed by DES imparts a significant importance in further tailoring the insulating property of non-plasticized polymer electrolytes, CA-0. The addition of DES promotes high dissociation of LiTFSI in CA matrix through weakening the inter-ion Coulombic force that holds together the two different charged ions, forming free ions of Li^+ and $TFSI^-$. Hence, more number of free mobile Li^+ and $TFSI^-$ ions will be available to participate in ion conduction upon increasing DES plasticization.

Another justification supporting the enhancement in ionic conductivity with increasing DES content is attributed to the increase in the number of transit site, in this case it is referred to the chloride ion (Cl^-) obtained upon miscibility of DES in the CA matrix. This transit site acts as an alternative pathway for the hopping of Li^+ ions along the polymer chain when there is no availability of vacant oxygen in CA polymer backbone to form coordination (Yahya et al., 2006). Herewith, the mobility of Li^+ ions is assured. Nevertheless, this alternative pathway shortens the Li^+ ions hopping distance from one vacant site to another and thus more frequent Li^+ ions transportation is expected to occur.

3.1.2. Influence of the storage time

Incorporation of DES in polymer electrolytes is believed to improve the aging effect. In order to justify the mentioned statement, the ionic conductivity of selected samples was monitored at room temperature for the duration of 30 days. The collected results are plotted in Fig. 1 for the samples of CA-0, CA-20, CA-40 and CA-60 respectively at room temperature.

From Fig. 1 it is observed that the sample CA-0 experiences greatest decrease in ionic conductivity with time compared to the DES-plasticized polymer electrolytes. This concludes that CA-0 does not have the tendency to retain ionic conductivity for a longer duration. This is due to the presence of low concentration of amorphous phase in the CA-0, which gives rise to less availability of polar functional groups to retain the liquid components within the membrane structure. Thus, the ionic conductivity decreases over time through the dissipation of liquid component from the matrix.

In view of the results for CA-20, CA-40 and CA-60, the ionic conductivity is further retained over time as increase in DES content. This is due to the increase in the polar functional groups that have higher liquid retention capabilities (Ramesh & Arof, 2009). So upon increasing doping of DES more liquid components are trapped within the CA membrane structure which possess fewer tendencies for the DMF volume are dissipated out. Thus, the ionic conductivity is retained with time as increase in DES plasticization. There is no significant change in the ionic conductivity is observed after 10 days in all the tested samples. This reveals that the samples retain high chemical integrity overcoming the liquid leakage limitation over the storage time.

The increase in DES content in the polymer electrolytes considerably increases the number of available polar sites in the CA:LiTFSI:DES matrix, which is evident through its capability in retaining the ionic conductivity over the storage time. Sample CA-60 appears as the highest conducting sample and has high tendency in retaining the ionic conductivity from 2.61×10^{-3} S cm^{-1} (after casting) to 5.89×10^{-5} S cm^{-1}, even after the storage time of 30 days. This is due to the high presence of polar functional groups that have high liquid retention capabilities.

Table 2
Band assignments and wavenumbers of some important peaks in FTIR spectra exhibited by pure constituents.

Sample	Band assignments	Wavenumber (cm^{-1})
CA	O—H stretching	3445
	C—H stretching (CH_3)	2932
	C—H stretching (CH_2)	2879
	C=O symmetric	1734
	C=O asymmetric	1656
	CH_2 bending	1436
	δC—H bending	1369
	C—O—C asymmetric bridge stretching	1158
	C—O—C stretching of the pyrose ring	1032
	δC—H	901
LiTFSI	O—H	3419
	S—CH_3	2979 and 2876
	C—SO_2—N	1356
	—CF_3	1193
	C—F stretch	1142
	S=O	1065
DES	C—H stretching (CH_3)	2964
	C—H stretching (CH_2)	2873
	C=O	1643
	Ammonium ion	1169

3.2. FTIR-HATR studies

FTIR spectroscopy is a reliable and well recognized fingerprinting technique used in detecting the complexation between the constituents that present in both crystalline and amorphous phases. The occurrence of complexation can be deduced by relying on the alternations in the cage peaks in terms of the wavenumber shifting, shape, relative intensity, disappearance of existing peak and even through the formation of new peaks. The FTIR spectra of polymer electrolytes vary according to their compositions and it is independent of concentration. The band assignments of pure substances: CA, LiTFSI and DES are summarized in Table 2 (da Conceiçao, Lucena, de Alencar, Mazzeto, & de Soares, 2003; Ramesh & Lu, 2008).

The occurrence of complexation between pure CA and pure LiTFSI was confirmed based on the alternations in CA-0 spectrum as depicted in Fig. 2. In pure CA, the peak at 1734 cm^{-1} was shifted to lower wavenumber of 1726 cm^{-1} in CA-0 after complexation

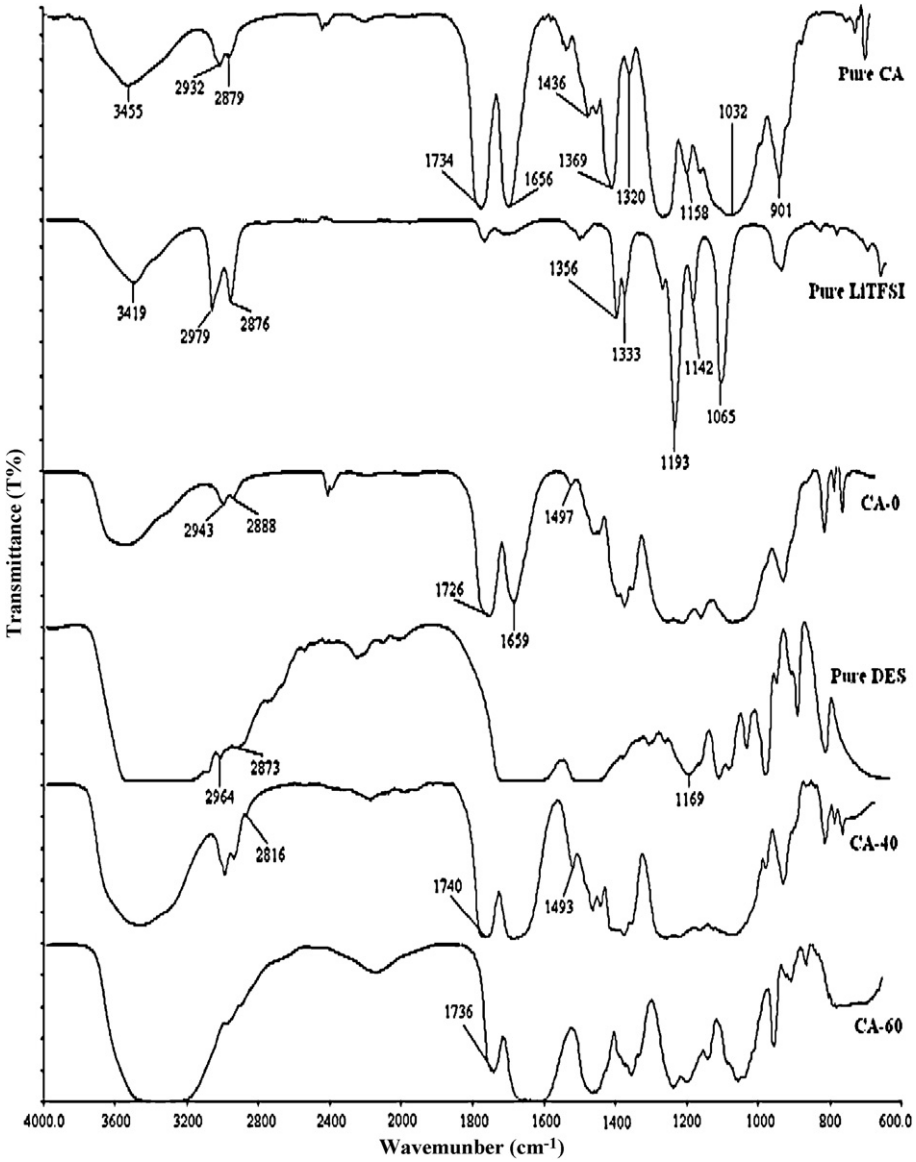

Fig. 2. FTIR spectra of pure CA, pure LiTFSI, pure DES, CA-0, CA-40 and CA-60 in transmittance mode.

with LiTFSI. This evidences the dissociation of Li^+ ion from LiTFSI, which then forms co-ordination with the electron donor oxygen atoms in polymer backbone. This interaction consequently results in the reduction in peak relative intensity from 64% (pure CA) to 55% (CA-0) as shown in Fig. 3. The complexation between these two pure constituents was further supported by the absence of peak at 1320 cm^{-1} in pure CA upon addition of LiTFSI. The disappearance of peak proves the breaking of —Ac from the —OAc functional group, allowing the oxygen to be unoccupied in order to behave as a transit site for the mobility of Li^+ ions.

A simple peak overlapping between the single intense peak at 1369 cm^{-1} in pure CA with two peaks at 1356 and 1333 cm^{-1} in pure LiTFSI results in three peaks formation at 1367, 1348 and 1325 cm^{-1} in CA-0. The observed change in the shape of peak is another evidence to prove the complexation. The peak that co-exists at 1656 cm^{-1} in pure CA was displaced to 1659 cm^{-1} in CA-0 with a reduced relative intensity from 61% to 47% upon complexation with LiTFSI. The occurrence of complexation between CA and LiTFSI was further been verified by the band broadening effect at the wavenumber range of 1030–1250 cm^{-1} in CA-0, which is due to the peak overlapping. The above discussed changes in the cage peaks indicate the occurrence of complexation between CA and LiTFSI.

The incorporation of DES in CA:LiTFSI matrix forms some degree of complexation. This can be clearly observed from the FTIR spectrum of samples CA-40 and CA-60 in Fig. 2. In CA-0, the peak present at 1497 cm^{-1} was displaced to 1493 cm^{-1} upon incorporation of 40 wt.% DES and with further addition of 60 wt.% DES this peak disappears. These observations suggest that some degree of complexation occurred when a different DES content is incorporated in CA:LiTFSI:DES polymer electrolytes.

The occurrence of complexation can further been proved by relying on the C=O characteristic peak present at 1726 cm^{-1} in CA-0. This peak is shifted to 1740 cm^{-1} and 1736 cm^{-1} respectively in CA-40 and CA-60 upon complexation with increasing DES particles. The initial displacement of the reference peak to a higher wavenumber upon the addition of 40 wt.% DES is attributed to the weaker interaction between the mobile Li^+ ions and double bonded oxygen group; probably the mobile Li^+ ions favorably form the interaction with the free moving transit sites created by the DES at this composition. Nevertheless this peak is found to be shifted to

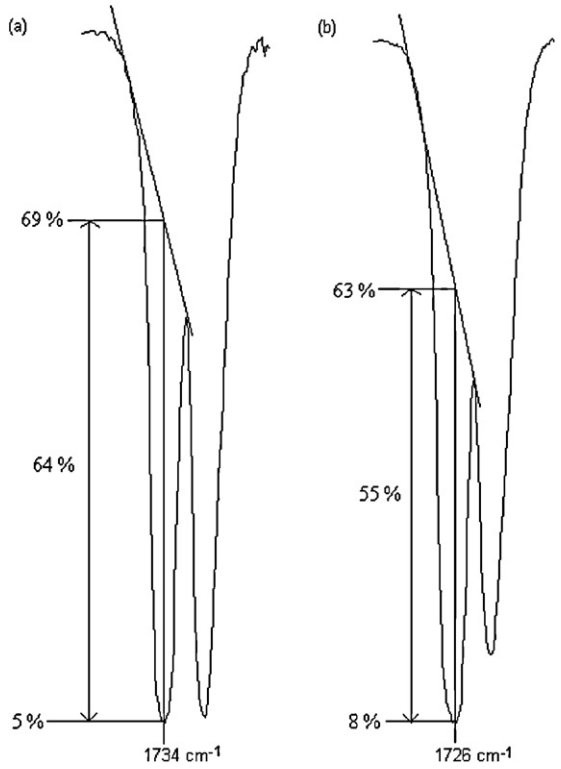

Fig. 3. The changes in intensity of C=O symmetric band for (a) pure CA and (b) CA-0.

a lower wavenumber as more DES particles are being incorporated, which is imposed by the presence of high concentration of mobile Li^+ ions which may also form interaction with the C=O group when the neighboring DES transit sites are being occupied. This greater interaction is then induces to the displacement of the C=O characteristic peak to a lower wavenumber. Besides that, decrease in the relative intensity of the reference peak is also being observed, which is reduced from 55% (CA-0) to 45% (CA-40) and finally to 38% (CA-60).

The complexation can also been confirmed based on the two moderate peaks that co-exist at 2943 cm^{-1} and 2888 cm^{-1} in CA-0, which become more intense and a shoulder forms at 2816 cm^{-1} upon addition of 40 wt.% DES into the non-plasticized sample. This cage peaks were consequently found to flatten at the highest DES content (CA-60). Other evidence of complexation was based on the peak at 1659 cm^{-1} in CA-0, which subsequently broadens as the DES content is increased in CA-0, implying the greater involvement of oxygen atom (C=O asymmetric) in forming co-ordination with increasing number of Li^+ ions.

Based on the observed changes in the FTIR cage peak it can be justified that some degree of co-ordination or complexation occurred among CA, LiTFSI and DES. The similarity between the FTIR spectrums of each tested samples indicates that the LiTFSI and DES are physically bonded with CA.

3.3. XRD analysis

X-ray diffraction analysis was executed to monitor the changes in the structural properties of the polymer electrolytes as different amount of DES is incorporated in the CA:LiTFSI:DES matrix. This is a versatile technique used for phase identification of a material that is available in both crystalline and amorphous regions. This analysis aids in explaining the exerted ionic conductivity trend.

Fig. 4a depicts the diffraction patterns of pure CA present in two different forms: powder and thin film. Based on the XRD pattern

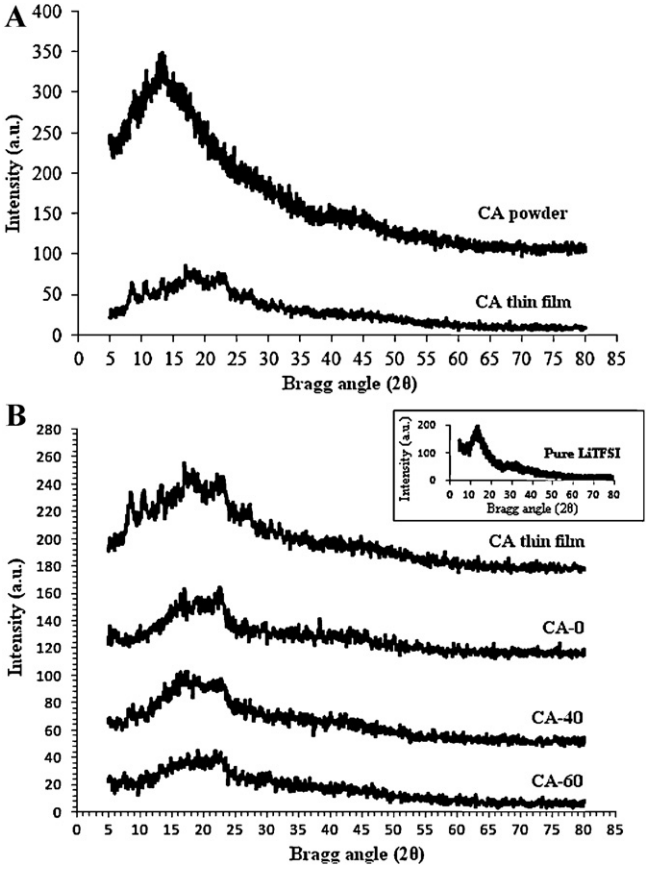

Fig. 4. XRD patterns of (a) pure CA that present in two different states: powder and thin film and (b) pure CA-thin film, CA-0, CA-40 and CA-60.

of powder CA, observation of an intense diffraction peak centered at $2\theta = 13.5^\circ$ reveals the crystalline nature of CA powder. This peak becomes less prominent after the CA powder is processed into thin film, this reveals the suppression of crystallinity in CA powder. Some degree of crystallinity in the CA thin film sample still persists, evidence through the observation of moderate peaks at the angles $2\theta = 8.5^\circ$, 10.5°, 13.5°, 17.5° and 23.5° within the hump diffraction peak. The observation of both crystalline and amorphous phase in the thin film makes it to be present in semi-crystalline nature. Based on the above, it is clear that the first structural disorderliness occurs when the CA powder is dissolved in the DMF solvent to process it into thin film.

In order to further understand the structural conversion that takes place in the matrix, a few selected samples with the doping of LiTFSI and different DES content were subjected to this analysis. Fig. 4b depicts the diffraction patterns of pure CA (thin film), pure LiTFSI, CA-0, CA-40 and CA-60 at room temperature.

The inset graph represents the XRD pattern of pure LiTFSI, which reveals the crystalline nature of this compound based on the existence of a single intense diffraction peak centered at $2\theta = 13.5^\circ$. This peak was found to be absent in CA-0 due to the complete dissolution of LiTFSI in the CA matrix (Sharma & Sekhon, 2007). The complete dissolution induces an increase in the CA matrix amorphous region, evidence through the disappearance of moderate peaks that initially present at $2\theta = 8.5^\circ$, 10.5° and 13.5°. The substantial broadening in the CA-0 diffraction peak is another evidence to support the disruption in the CA crystallinity upon complexation with LiTFSI.

The semi-crystalline nature CA:LiTFSI matrix was further being disrupted upon addition of DES. This was confirmed by the substantial broadening in the diffraction peak at the angle ranging from 5° to 30° in the DES plasticized samples (CA-40 and CA-60). It was

noted that as the percentage of DES in the polymer electrolyte increases from 40 wt.% to 60 wt.% the intensity of the diffraction peak decreases with a substantial increase in broadness. This observation marks the decline in the degree of crystallinity in CA matrix as more DES content is incorporated in the CA:LiTFSI:DES matrix.

Further illustration on the suppression of crystallinity is based on the two diffraction peaks assigned at $2\theta = 17.5^\circ$ and 23.5° in CA-40. The incorporation of additional 20 wt.% DES in CA-40 alters the shape of the diffraction peak at $2\theta = 17.5^\circ$ (CA-40) to a slight shoulder, as shown in CA-60. This observation illustrates that further structural conversion takes place at this angle and more amorphous region is available for the movement of Li^+ ions. Some degree of crystallinity in CA still persists even at the highest conducting composition, as observed from the distinct peak at $2\theta = 23.5^\circ$. This reveals that the system is not fully amorphous yet attains high ionic conductivity due to the reduction in the intensity of the CA crystallization peak from a hump shape (in CA powder) to a broadening shape upon addition of LiTFSI and DES. The observed changes in the diffraction peak also provide an insight on the occurrence of complexation among CA, LiTFSI and DES that takes place in the amorphous region (Ramesh et al., 2010).

From this analysis, it is found that the reduction in CA matrix's crystallinity is caused by the structural reorganization imposed by DES. This structural reorganization subsequently induces greater presence of amorphous phase in the polymer electrolytes matrix. This allows fast acceleration of Li^+ ions mobility and progressively increases the ionic conduction. Based on this analysis, it is found that the sample CA-60 possesses high concentration of amorphous phase. This permits high mobility of Li^+ ions to take place within the matrix. Thus, CA-60 appears as the highest conducting sample concurrent with earlier findings.

3.4. TGA analysis

The changes in the thermal properties of CA:LiTFSI:DES matrix upon doping with different DES content are studied for the samples of pure CA, CA-0, CA-40 and CA-60 with reference to Fig. 5, which is the combination plot of TGA and DTG curves. The advantage of combining the DTG graph with the TGA results is to provide a clearer observation at which temperature the samples underwent decomposition stages. This is because most of the decomposition stages occurring in the plasticized matrix are undetectable in the TGA curves since these natured samples have several numbers of decomposition stages.

The TGA technique detects the degradation mechanism of polymer electrolytes which occurs in two main processes: dehydration and decomposition, upon subjecting the samples with continuous heating. Dehydration is the initial weight loss process occurring at the temperature of 100 °C where the trapped liquid components; residual solvent or moisture, in the polymer electrolytes matrix are being evaporated out (Mohamad & Arof, 2007). With further increase in the temperature beyond 100 °C the decomposition of polymer electrolytes starts to take place, in which the resultant weight loss is attributed to the depolymerization of the long polymer chain. The percentages of weight loss observed at this stage are in greater amount compared to the weight loss observed during the dehydration process.

In this communication, the alternation in the thermal properties of the developed matrix upon doping with LiTFSI and DES is studied with reference to the decomposition process. The information on the decomposition temperatures and percentage total weight loss of all the tested polymer electrolytes is listed in Table 3.

The decomposition process provides information on the thermal behavior of polymer electrolytes in terms of the heat-resistivity and thermal stability. The term heat-resistivity accounts to the ability of the chains in the polymer electrolyte matrix to retain its original form upon subjecting to continuous heating. This property is studied by referring to the samples final decomposition temperature. Upon achieving the decomposition temperature of polymer electrolyte the sample becomes heat sensitive and undergoes structural deformation. This yields to the observation of weight loss as the sample loses its thermal stability.

Table 3
The decomposition temperature and percentage total weigh loss.

Sample	Decomposition temperature, T_d (°C)			Total weight loss (wt.%)
	First	Second	Third	
Pure CA	363.40	–	–	88
CA-0	293.30	414.01	–	84
CA-40	256.75	309.57	407.19	77
CA-60	256.45	310.97	377.81	90

Based on the DTG curves, it is observed that pure CA, CA-0 and DES-plasticized samples undergo one-step, two-steps and three-steps of decomposition process respectively. The number of decomposition steps exhibited by samples is dependent on how many different natured additives present in the matrix. This is because different natured additives decompose at different temperatures. As for the membrane made of pure CA it is found to decompose at the temperature of 363.40 °C. At this temperature the glucose monomers that initially build up the CA detach from the long polymer chain and at progressive heating carbonization, ash is formed (Mano, Koniarova, & Reis, 2003).

When the CA matrix is doped with LiTFSI two-step decomposition processes is observed, in which the first and second decomposition processes correspond to the decomposition of CA polymer and organic part in LiTFSI respectively. The decrease in the first decomposition temperature of CA-0 in comparison with the decomposition temperature of pure CA illustrates the disruption in the CA crystalline structure upon complexation with LiTFSI. This disruption gives rise to the presence of amorphous fraction in the CA matrix thus the weakly bonded molecules presenting in this region can be easily decompose at lower temperature. Nevertheless, the heat-resistivity of CA-0 is found to enhance due to the presence of organic part in LiTFSI which formulates this composition to be more heat-stable and thus lessen the total weight loss. This makes the CA-0 matrix to have improved thermal stability compared to pure CA.

The thermal profile of the CA:LiTFSI matrix is tailored upon addition of DES into the matrix. The DES-plasticized matrix exhibited three-step decomposition: first, second and third respectively corresponds to the decomposition process of CA polymer, organic part in DES and organic part in LiTFSI. Upon complexation with DES the first decomposition temperature of CA-40 and CA-60 is shifted to a lower range compared to CA-0. This is due to the unusual solvent property govern by DES that further weakens the interaction between the chains present in CA matrix in greater extent compared to LiTFSI and ultimately causes greater structural disorderliness. The presence of high concentration of amorphous phase allows the polymer electrolytes to decompose at lower temperature when subjected to minimum amount of heat. Therefore, it can be noted that the addition of DES in polymer electrolyte makes the matrix looses its resistivity towards heat and gradually decreases the first decomposition temperature.

The second decomposition temperature corresponds to the decomposition of DES particles which is found to fall around the same temperature in both CA-40 and CA-60. The DES particles exhibited change in the matrix's thermal behavior by causing disruption in the CA crystallinity. The third decomposition step in the DES-plasticized sample is found to occur at lower temperature with increasing addition of DES particles compared to CA-0.

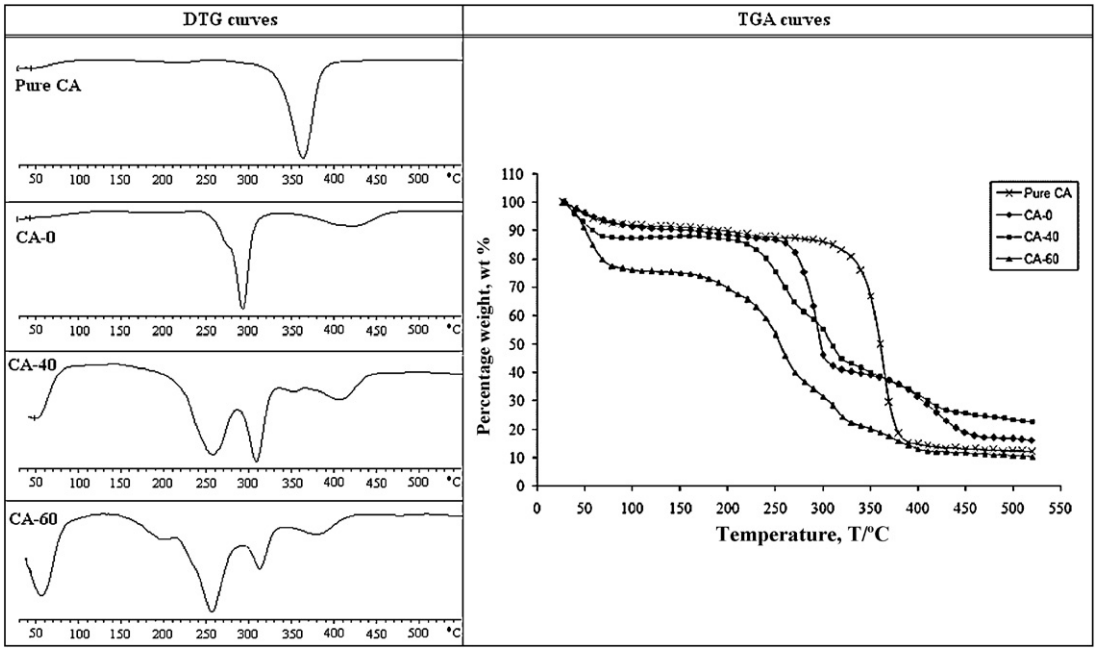

Fig. 5. Combination plots of DTG and TGA curves of pure CA, CA-0, CA-40 and CA-60.

This is attributed to the high presence of free organic groups of LiTFSI as the DES effectively breaks the bond connecting the different charged ions. Thus, the free organic groups decompose at lower temperature as increasing doping of DES in the matrix and ultimately decrease the heat-resistivity.

Comparison on the thermal stability between CA-40 and CA-60 reveals the improvement in this property only at the initial addition of 40 wt.% DES, evident by the reduction in total weight loss. The initial improvement is associated with the presence of organic part in DES which only decomposes completely at a very high temperature. Herewith, less components being detached from the matrix making the polymer electrolytes more thermally stable. As the DES content increases, the effect of greater structural disorderliness in the CA matrix overshadows the effect imposed by the organic part in DES. This makes the matrix to be thermally unstable and thus decomposes at lower temperature.

Overall, it is found that the DES-plasticized sample is more heat-stable compared to pure CA. Hence, with the presence of an appropriate DES content in the CA:LiTFSI:DES, a matrix with an acceptable thermal properties can be formulated to well support the applications of electronic devices.

4. Conclusion

Biodegradable thin film polymer electrolytes were developed by plasticizing the CA:LiTFSI:DES matrix with up to 60 wt.% DES. The highest plasticized sample CA-60 exhibits the highest ionic conducting and has the greatest ability to retain the property even after 30 days of storage with the value of 5.89×10^{-5} S cm^{-1}. This is attributed to its high chemical integrity (no liquid leakage). The changes in the matrix properties upon different DES ratio addition are induced by the possible interactions between the added chemical constituents as confirmed from the FTIR spectra. This interaction induces to structural disorderliness through the observation of reduced intensity of XRD diffraction peaks. The thermal profile of the matrix is also been tailored upon increasing addition of DES content. With increase in DES content the samples thermal-resistivity decreases while an enhancement in the thermal stability is observed at the minimum DES addition. As a conclusion, the developed polymer electrolytes best suits for the electrochemical applications due to its high conducting nature, thermally stable than the pure CA and environmental-friendly.

Acknowledgements

The co-author named R. Shanti gratefully acknowledges the "Skim Bright Sparks University Malaya (SBSUM)" for the financial support. This work was supported by the Exploratory Research Grant Scheme (ERGS: ER017-2011A).

References

Abbott, A. P., Capper, G., Davies, D. L., Rasheed, R. K., & Tambyrajah, V. (2003). Novel solvent properties of choline chloride/urea mixtures. *Chemical Communications*, *39*, 70–71.

Armand, M. B. (1986). Polymer electrolytes. *Annual Review of Materials Science*, *16*, 245–261.

Averous, L., Fringant, C., & Moro, L. (2001). Plasticized starch–cellulose interactions in polysaccharide composites. *Polymer*, *42*, 6565–6572.

da Conceiçao, M., Lucena, C., de Alencar, A. E. V., Mazzeto, S. E., & de Soares, S. (2003). The effect of additives on the thermal degradation of cellulose acetate. *Polymer Degradation Stability*, *80*, 149–155.

Hou, Y., Gu, Y., Zhang, S., Yang, F., Ding, H., & Shan, Y. (2008). Novel binary eutectic mixtures based on imidazole. *Journal of Molecular Liquids*, *143*, 154–159.

Jhong, H.-R., Wong, D. S.-H., Wan, C.-C., Wang, Y.-Y., & Wei, T.-C. (2009). A novel deep eutectic solvent-based ionic liquid used as electrolyte for dye-sensitized solar cells. *Electrochemistry Communications*, *11*, 209–211.

Mano, J. F., Koniarova, D., & Reis, R. L. (2003). Thermal properties of thermoplastic starch/synthetic polymer blends with potential biomedical capability. *Journal of Materials Science: Materials in Medicine*, *14*, 127–135.

Mohamad, A. A., & Arof, A. K. (2007). Plasticized alkaline solid polymer electrolyte system. *Materials Letters*, *61*, 3096–3099.

Rajendran, S., Sivakumar, M., & Subadevi, R. (2004). Investigations on the effect of various plasticizers in PVA–PMMA solid polymer blend electrolytes. *Materials Letters*, *58*, 641–649.

Ramesh, S., & Lu, S.-C. (2008). Effect of nanosized silica in poly(methyl methacrylate)–lithium bis(trifluoromethanesulfonyl)imide based polymer electrolytes. *Journal of Power Sources*, *185*, 1439–1443.

Ramesh, S., Tai, F. Y., & Chia, J. S. (2008). Conductivity and FTIR studies on PEO–LiX [X: $CF_3SO_3^-$, SO_4^{2-}] polymer electrolytes. *Spectrochimica Acta Part A*, *69*, 670–675.

Ramesh, S., & Arof, A. K. (2009). A study incorporating nano-sized silica into PVC-blend-based polymer electrolytes for lithium batteries. *Journal of Materials Science*, *44*, 6404–6407.

Ramesh, S., Teh, G. B., Louh, R.-F., Hou, Y. K., Sin, P. Y., & Yi, L. J. (2010). Preparation and characterization of plasticized high molecular weight PVC based polymer electrolytes. *Sadhana*, *35*, 87–95.

Ratner, M. A., & Shriver, D. F. (1988). Ion transport in solvent-free polymers. *Chemical Reviews*, *88*, 109–124.

Sharma, J. P., & Sekhon, S. S. (2007). Nanodispersed polymer gel electrolytes: Conductivity modification with the addition of PMMA and fumed silica. *Solid State Ionics*, *178*, 439–445.

Shriver, D. F., Papke, B. L., Ratner, M. A., Dupon, R., Wong, T., & Brodwin, M. (1981). Structure and ion transport in polymer–salt complexes. *Solid State Ionics*, *5*, 83–88.

Siva Kumar, J., Subrahmanyam, A. R., Jaipal Reddy, M., & Subba Rao, U. V. (2006). Preparation and study of properties of polymer electrolyte system (PEO + $NaClO_3$). *Materials Letters*, *60*, 3346–3349.

Swatloski, R. P., Spear, S. K., Holbrey, J. D., & Rogers, R. D. (2002). Dissolution of cellulose with ionic liquids. *Journal of American Chemical Society*, *124*, 4974–4975.

Uma, T., Mahalingam, T., & Stimming, U. (2003). Mixed phase solid polymer electrolytes based on poly (methylmethacrylate). *Materials Chemistry and Physics*, *82*, 478–483.

Wu, R.-L., Wang, X.-L., Li, F., Li, H.-Z., & Wang, Y.-Z. (2009). Green composite films prepared from cellulose, starch and lignin in room-temperature ionic liquid. *Bioresource Technology*, *100*, 2569–2574.

Yahya, M. Z. A., Ali, A. M. M., Mohammat, M. F., Hanafiah, M. A. K. M., Mustaffa, M., Ibrahim, S. C., et al. (2006). Ionic conduction model in salted chitosan membranes plasticized with fatty acid. *Journal of Applied Sciences*, *6*, 1287–1291.

Zhang, J., Wu, T., Chen, S., Feng, P., & Bu, X. (2009). Versatile structure-directing roles of deep eutectic solvents and their implication in generation of porosity and open metal sites for gas storage. *Angewandte Chemie International Edition in English*, *48*, 3486–3490.